Abe K, Machida T, **Sumitomo N**, Yamamoto H, Ohkubo K, Watanabe I, **Makiyama T**, Fukae S, Kohno M, Harrell D T, Ishikawa T, Tsuji Y, Nogami A, Watabe T, Oginosawa Y, Abe H,	Sodium channelopathy underlying familial sick sinus syndrome with early onset and predominantly male characteristics.	Circ Arrhythm Electrophysiol.	7(3)	511-7	2014
Abe Y, **Sumitomo N**, Okuma H, Nakamura T, Fukuhara J, Ichikawa R, Matsumura M, Miyashita M, Kamiyama H, Ayusawa M, Watanabe M, Joo K, **Makita N**, **Horie M.**	Successful control of life-threatening polymorphic ventricular tachycardia by radiofrequency catheter ablation in an infant.	Heart Vessels.	29(3)	422-6	2014
Kinoshita K, Komatsu T, Nishide K, Hata Y, Hisajima N, Takahashi H, Kimoto K, **Aonuma K**, Tsushima E, Tabata T, Yoshida T, Mori H, Nishida K, Yamaguchi Y, Ichida F, Fukurotani K, Inoue H, Nishida N.	A590T mutation in KCNQ1 C-terminal helix D decreases IKs channel trafficking and function but not Yotiao interaction.	J Mol Cell Cardiol.	72	273-80	2014
Kusumoto S, Kawano H, **Makita N**, Ichimaru S, Kaku T, Haruta D, Hida A, Sera N, Imaizumi M, Nakashima E, Maemura K, Akahoshi M.	Right bundle branch block without overt heart disease predicts higher risk of pacemaker implantation: The study of atomic-bomb survivors.	Int J Cardiol.	174 (1)	77-82	2014
Ohno S, Omura M, Kawamura M, Kimura H, Itoh H, **Makiyama T**, Ushinohama H, **Makita N**, **Horie M**.	Exon 3 deletion of RYR2 encoding cardiac ryanodine receptor is associated with left ventricular non-compaction.	Europace.	16 (11)	1646-54	2014
Yoshida M, Ando S, Chishaki A, **Makita N**, Hasegawa Y, Narita S, Momii H, Kadokami T.	Normal dose of pilsicainide showed marked negative inotropic effects in a patient who had no underlying heart disease.	J Arrhythmia.	30(1)	68-70	2014
Tsuji Y, Ishikawa T, **Makita N**.	Molecular mechanisms of heart failure progression associated with implantable cardioverter-defibrillator shocks for ventricular tachyarrhythmias.	J Arrhythmia.	30(4)	235-241	2014
Seki A, Nishii K, **Hagiwara N**.	Gap junctional regulation of pressure, fluid force, and electrical fields in the epigenetics of cardiac morphogenesis and remodeling.	Life Sciences	pii: S0024-3205(14)	00902-3	2014

Ejima K, Kato K, Arai K, Fukushima K, Fukushima N, Suzuki T, Yoshida K, Nuki T, Uematsu S, Hoshi H, Manaka T, Ashihara K, Shoda M, **Hagiwara N**.	Impact of atrial remodeling on the outcome of radiofrequency catheter ablation of paroxysmal atrial fibrillation.	Circulation Journal	78(4)	872-877	2014
Fukushima N, Tsurumi Y, Jujo K, Gomita K, Sekiguchi H, Honda A, Yumino D, Kawana M, **Hagiwara N**.	Impact of myocardial reperfusion status on QT dispersion after successful recanalization of the infarct-related artery in acute myocardial infarction.	Journal of interventional cardiology	27(3)	252-259	2014
Yashiro B, Minami Y, Terajima Y, **Hagiwara N**.	Prognostic difference between paroxysmal and non-paroxysmal atrial fibrillation in patients with hypertrophic cardiomyopathy.	Journal of Cardiology	63(6)	432-437	2014
Ejima K, Arai K, Suzuki T, Kato K, Yoshida K, Nuki T, Suzuki F, Uematsu S, Gomita K, Hoshi H, Manaka T, Ashihara K, Shoda M, **Hagiwara N**.	Long-term outcome and preprocedural predictors of atrial tachyarrhythmia recurrence following pulmonary vein antrum isolation-based catheter ablation in patients with non-paroxysmal atrial fibrillation.	Journal of Cardiology	64(1-2)	57-63	2014
Egashira T, Yuasa S, Kimura M, Sawano M, Anzai A, Hayashida K, Kawamura A, Kimura T, Nishiyama N, Aizawa Y, Takatsuki S, Tsuruta H, Murata M, Yamada Y, Kohno T, Maekawa Y, Sano M, Kosaki K, **Fukuda K**.	Coexistence of two distinct fascinating cardiovascular disorders: heterotaxy syndrome with left ventricular non-compaction and vasospastic angina.	Int J Cardiol.	174	e54-6	2014
Sano M, Aizawa Y, Katsumata Y, Nishiyama N, Takatsuki S, Kamitsuji S, Kamatani N, **Fukuda K**.	Evaluation of differences in automated QT/QTc measurements between Fukuda Denshi and Nihon Koden systems.	PLoS One.	9	e106947	2014
Aizawa Y, Sato M, Ohno S, **Horie M**, Takatsuki S, **Fukuda K**, Chinushi M, Usui T, Aonuma K, Hosaka Y, Haissaguerre M, Aizawa Y.	Circadian pattern of fibrillatory events in non-Brugada-type idiopathic ventricular fibrillation with a focus on J waves.	Heart Rhythm.	11	2261-6	2014
Yamakawa H, Murata M, Suzuki T, Yada H, Ishida H, Aizawa Y, Adachi T, Kamiya K, **Fukuda K**.	Suppression of Rad leads to arrhythmogenesis via PKA-mediated phosphorylation of ryanodine receptor activity in the heart.	Biochem Biophys Res Commun.	452	701-7	2014

Kaneko Y, **Horie M**, Niwano S, Kusano K, Takatsuki S, Kurita T, Mitsuhashi T, Nakajima T, Irie T, Hasegawa K, Noda T, **Kamakura S**, Aizawa Y, Yasuoka R, Torigoe K, Suzuki H, Ohe T, Shimizu A, **Fukuda K**, Kurabayashi M, Aizawa Y.	Electrical Storm in Patients with Brugada Syndrome is Associated with Early Repolarization.	Circ Arrhythm Electrophysiol.	7	1122-8	2014
Mitani Y, Ohta K Ichida F, Nii M, Arakaki Y, Ushinohama H, Takahashi T, Ohashi H, Yodoya N, Fujii E, Ishikura K, Tateno S, Sato S, Suzuki T, Higaki T, Iwamoto M, **Yoshinaga M,** Nagashima M, **Sumitomo**	Circumstances and Outcomes of Out-Of-Hospital Cardiac Arrest in Elementary and Middle School Students in the Era of Public-Access Defibrillation: Implications for Emergency Preparedness in Schools.	Circ J.	78(3)	701-7	2014
Nakamura A, **Horigome H**, Seo Y, Ishizu T, Sumazaki R.	Right ventricular remodeling due to pulmonary regurgitation is associated with reduced left ventricular free wall strain in surgically repaired tetralogy of fallot.	Circ J	78(8)	1960-6	2014
Horigome H	Current status and future direction of cardiac resynchronization therapy for congenital heart disease and pediatric patients.	Circ J	78(7)	1579-81	2014
Murakami T, **Horigome H**, Shiono J, Ishiodori T, Ban Y, Gomi S, Abe M.	Prenatal Diagnosis of Congenital Absence of Aortic Valve: A Report of Two Cases with Different Outcomes and a Literature Review.	Fetal Diagn Ther.		Epub	2014
Sumitomo N	Device therapy in Children and Patients with Congenital Heart disease	J Arrhythmia	30(6)	428-432	2014
Sumitomo N	E1784K Mutation in *SCN5A* Gene and Overlap Syndrome	Circ J	78(8)	1839 – 1840	2014
Abe Y, **Sumitomo N**, Okuma H, Nakamura T, Fukuhara J, Ichikawa R, Matsumura M, Miyashita M, Kamiyama H, Ayusawa M, Watanabe, M Joo K, **Makita N**, **Horie M**	Successful Control of Life Threatening Polymorphic Ventricular Tachycardias by Radiofrequency Catheter Ablation in an Infant	Heart	29	422-6	2014

Noto N, Kamiyama H, Karasawa K, Ayusawa M, **Sumitomo N**, Okada T, Takahashi S	Long-term prognostic impact of dobutamine stress echocardiography in patients with Kawasaki disease and coronary artery lesions: A 15-year follow-up study	J Am Coll Cardiol	63(4)	337-44	2014
Suzuki T, **Sumitomo N**, Yoshimoto J, **Miyazaki A**, Hinokiyama K, Ushinohama H, Yasukochi S	Current Trends in Use of Implantable Cardioverter Defibrillators and Cardiac Resynchronization Therapy With a Pacemaker or Defibrillator in Japanese Pediatric Patients	Circ J	78(7)	1710 - 1716	2014
Morita H, Zipes DP, Morita ST, Wu J.	Isolation of canine coronary sinus musculature from the atria by radiofrequency catheter ablation prevents induction of atrial fibrillation.	Circulation. Arrhythmia and Electrophysiology.	7	1181-1188	2014
Nagase S, Banba K, Nishii N, **Morita H**, Fukushima Kusano K, Ohe T, Ito H.	Multiform premature ventricular contractions and polymorphic ventricular tachycardia caused by purkinje activity with slow conduction in idiopathic ventricular fibrillation.	Intern Med.	53	725-728	2014
Nakagawa K, Nagase S, **Morita H**, Ito H.	Left ventricular epicardial electrogram recordings in idiopathic ventricular fibrillation with inferior and lateral early repolarization.	Heart Rhythm	11	314-317	2014
Tokioka K, Kusano KF, **Morita H**, Miura D, Nishii N, Nagase S, Nakamura K, Kohno K, Ito H, Ohe T.	Electrocardiographic parameters and fatal arrhythmic events in patients with brugada syndrome: Combination of depolarization and repolarization abnormalities.	Journal of the American College of Cardiology.	63	2131-2138	2014
Kubo M, Miyoshi T, Kimura T, Noda Y, Kohno K, Nakamura K, **Morita H,** Ito H.	Add-on ezetimibe reduces small dense low-density lipoprotein cholesterol levels without affecting absorption of eicosapentaenoic acid in patients with coronary artery disease: A pilot study.	American journal of cardiovascular drugs: drugs, devices, and other interventions.	14	387-392	2014
Sakatani Y, Miyoshi T, Oe H, Noda Y, Ohno Y, Nakamura K, Saito Y, Osawa K, **Morita H**, Kohno K, Ito H.	Pioglitazone prevents the endothelial dysfunction induced by ischemia and reperfusion in healthy subjects.	Journal of cardiovascular pharmacology.	64	326-331	2014

Osawa K, Miyoshi T, Koyama Y, Hashimoto K, Sato S, Nakamura K, Nishii N, Kohno K, **Morita H**, Kanazawa S, Ito H.	Additional diagnostic value of first-pass myocardial perfusion imaging without stress when combined with 64-row detector coronary ct angiography in patients with coronary artery disease.	Heart	100	1008-1015	2014
Ohno Y, Miyoshi T, Noda Y, Oe H, Toh N, Nakamura K, Kohno K, **Morita H**, Ito H.	Bezafibrate improves postprandial hypertriglyceridemia and associated endothelial dysfunction in patients with metabolic syndrome: A randomized crossover study.	Cardiovascular diabetology.	13	71	2014
Osawa K, Miyoshi T, Koyama Y, Sato S, Akagi N, Morimitsu Y, Kubo M, Sugiyama H, Nakamura K, **Morita H**, Kanazawa S, Ito H.	Differential association of visceral adipose tissue with coronary plaque characteristics in patients with and without diabetes mellitus.	Cardiovascular diabetology	13	61	2014
Wang Q, Ohno S, Ding WG, Fukuyama M, Miyamoto A, Itoh H, **Makiyama T**, Wu J, Bai J, Hasegawa K, Shinohara T, Takahashi N, Shimizu A, Matsuura H, **Horie M**	Gain-of-function KCNH2 mutations in patients with Brugada syndrome	J Cardiovasc Electrophysiol	25(5)	522-30	2014
Fukuyama M, Wang Q, Kato K, Ohno S, Ding WG, Toyoda F, Itoh H, Kimura H, **Makiyama T,** Ito M, Matsuura H, **Horie M**	Long QT syndrome type 8: novel CACNA1C mutations causing QT prolongation and variant phenotypes.	Europace	12	1828-37	2014
Zhou J, Ding WG, **Makiyama T**, Miyamoto A, Matsumoto Y, Kimura H, Tarutani Y, Zhao J, Wu J, Zang WJ, Matsuura H, **Horie M**	A novel HCN4 mutation, G1097W, is associated with atrioventricular block	Circ J	78(4)	938-42	2014
Araki A, Katsuno M, Suzuki K, Banno H, Suga N, Hashizume A, Mano T, Hijikata Y, Nakatsuji H, **Watanabe H**, Yamamoto M, **Makiyama T**, Ohno S, Fukuyama M, Morimoto S, **Horie M**, Sobue G	Brugada syndrome in spinal and bulbar muscular atrophy.	Neurology	82(20)	1813-21	2014
Sato A, **Watanabe H,** Sonoda K, Chinushi M, Tsuda T, Izumi D, Furushima H, Minamino T.	Augmentation of the J wave by rapid pacing in a patient with vasospastic angina.	Int J Cardiol.	172	e111-113	2014

Yamada Y, Kinoshita H, Kuwahara K, Nakagawa Y, Kuwabara Y, Minami T, Yamada C, Shibata J, Nakao K, Cho K, Arai Y, Yasuno S, Nishikimi T, Ueshima K, **Kamakura S**, Nishida M, Kiyonaka S, Mori Y, Kimura T, Kangawa K, Nakao K.	A Inhibition of N-type Ca2+ channels ameliorates an imbalance in cardiac autonomic nerve activity and prevents lethal arrhythmias in mice with heart failure.	Cardiovasc Res.	104	183-93	2014
Ise T, Hasegawa T, Morita Y, Yamada N, Funada A, Takahama H, Amaki M, Kanzaki H, Okamura H, **Kamakura S**, **Shimizu W**, Anzai T, Kitakaze M.	Extensive late gadolinium enhancement on cardiovascular magnetic resonance predicts adverse outcomes and lack of improvement in LV function after steroid therapy in cardiac sarcoidosis.	Heart.	100	1165-72	2014
Takaya Y, Noda T, Nakajima I, Yamada Y, Miyamoto K, Okamura H, Satomi K, **Aiba T**, Kusano KF, Kanzaki H, Anzai T, Ishihara M, Yasuda S, Ogawa H, **Kamakura S**, **Shimizu W**.	Electrocardiographic predictors of response to cardiac resynchronization therapy in patients with intraventricular conduction delay.	Circ J.	78(1)	71-7	2014
Makita N, Yagihara N, Crotti L, Johnson CN, Beckmann BM, Roh MS, Shigemizu D, Lichtner P, Ishikawa T, **Aiba T**, Homfray T, Behr ER, Klug D, Denjoy I, Mastantuono E, Theisen D, Tsunoda T, Satake W, Toda T, Nakagawa H, Tsuji Y, Tsuchiya T, Yamamoto H, **Miyamoto Y**, Endo N, Kimura A, Ozaki K, Motomura H, Suda K, Tanaka T, Schwartz PJ, Meitinger T, Kääb S, Guicheney P, **Shimizu W**, Bhuiyan ZA, **Watanabe H**, Chazin WJ, George AL Jr.	Novel calmodulin mutations associated with congenital arrhythmia susceptibility.	Circ Cardiovasc Genet.	7(4)	466-74	2014
Aiba T, Farinelli F, Kostecki G, Hesketh GG, Edwards D, Biswas S, Tung L, Tomaselli GF	A mutation causing Brugada syndrome identifies a mechanism for altered autonomic and oxidant regulation of cardiac sodium currents.	Circulation Cardiovasc Genet.	7(3)	249-56	2014

Tokuyama T, **Nakano Y**, Awazu A, Uchimura-Makita Y, Fujiwra M, Watanabe Y, Sairaku A, Kajihara K, Motoda C, Oda N, Kihara Y.	Deterioration of the circadian variation of heart rate variability in Brugada syndrome may contribute to the pathogenesis of ventricular fibrillation.	J Cardiol.	64(2)	133-8	2014
Uchimura-Makita Y, **Nakano Y**, Tokuyama T, Fujiwra M, Watanabe Y, Sairaku A, Kawazoe H, Matsumura H, Oda N, Ikenaga H, Kajihara K, Motoda C, Oda N, Verrier R, Kihara Y.	Time-Domain T-Wave Alternans is Strongly Associated with a History of Ventricular Fibrillation in Patients with Brugada Syndrome.	J Cardiovasc Electrophysiol.	25(9)	1021-7	2014
Sairaku A, **Nakano Y**, Oda N, Uchimura Y, Tokuyama T, Kawazoe H, Fujiwara M, Watanabe Y, Matsumura H, Kihara Y.	Incomplete Cure of Tachycardia-Induced Cardiomyopathy Secondary to Rapid Atrial Fibrillation by Heart Rate Control Without Sinus Conversion.	J Cardiovasc Electrophysiol	25(10)	1037-43	2014
Sairaku A, **Nakano Y**, Kihara Y.	Does dabigatran interfere with intraablation heparinization?	Thromb Res	134(3)	742-3	2014
Sairaku A, Yoshida Y, Hirayama H, **Nakano Y**, Kihara Y.	Impact of pulmonary vein isolation on fractionated atrial potentials and ganglionated plexi in patients with persistent atrial fibrillation.	Int Heart J	55(6)	494-8	2014
辻 幸臣, 蒔田直昌	重症不整脈 electrical storm：基礎研究からのアプローチ	長崎市医師会報	48	7-11	2014
蒔田直昌	遺伝性不整脈の遺伝子診断の歴史	呼吸と循環	62	827-831	2014
住友直方	小児不整脈の診断ガイドライン	小児内科	47(2)	247-254	2015
三好剛一、前野泰樹、左合治彦、稲村 昇、安河内聰、川滝元良、 **堀米仁志**、与田仁志、竹田津未生、生水真紀夫、新居正基、賀藤均、萩原聡子、尾本暁子、**白石 公**、坂口平馬、西村邦宏、上田恵子、桂木真司、池田智明	治療困難症例から学ぶ 心構造異常を伴う胎児徐脈性不整脈についての検討 胎児徐脈の胎児治療に関する現状調査 2002-2008 より	日本周産期・新生児医学会雑誌	50(1)	136-8	2014
住友直方	刺激伝導系の発達	心臓	46(2)	156-161	2014

住友直方	先天性心疾患における不整脈治療の最前線	循環器内科	75(1)	52-58	2014
住友直方	小児不整脈の学校生活管理指導ガイドライン（2013）	小児科	55(1)	55-54	2014
住友直方	小児循環器専門医のための総説、学校心臓検診	日本小児循環器学会誌	30(1)	11-21	2014
住友直方	頻拍性不整脈	小児科診療	77	378-381	2014
住友直方	心室頻拍、心室細動	小児内科	46	366-373	2014
杉山洋樹、森田　宏	遺伝性不整脈の病態に基づいた薬物治療	呼吸と循環	62	841-846	2014
上岡　亮、森田　宏	Brugada 症候群、進行性伝導障害（PCCD）	Cardiac Practice	25	105-109	2014
上岡　亮、森田　宏	合併症のある高血圧症例のβ遮断薬：不整脈・心臓突然死	血圧	21	764−767	2014
中川晃志、永瀬　聡、和田匡史、田中正道、西井伸洋、寒川睦子、河野晋久、中村一文、森田　宏、草野研吾、伊藤　浩、湯本晃久、向原直木、大江透	左室側壁心外膜側に不整脈基質が存在すると考えられたJ波症候群の1例.	臨床心臓電気生理	37	127-135	2014
林　研至、山岸正和	家族性心房細動	循環器科	75	499	2014

Ⅳ. 研究成果の刊行物・別刷

A *KCNQ1* mutation contributes to the concealed type 1 long QT phenotype by limiting the Kv7.1 channel conformational changes associated with protein kinase A phosphorylation

Daniel C. Bartos, PhD,[*] John R. Giudicessi, BA,[†] David J. Tester, BS,[†] Michael J. Ackerman, MD, PhD,[†] Seiko Ohno, MD, PhD,[‡] Minoru Horie, MD, PhD,[‡] Michael H. Gollob, MD,[§] Don E. Burgess, PhD,[*] Brian P. Delisle, PhD[*]

From the [*]Department of Physiology, Center for Muscle Biology, University of Kentucky, Lexington, Kentucky, [†]Departments of Medicine, Pediatrics, and Molecular Pharmacology and Experimental Therapeutics, Divisions of Cardiovascular Diseases and Pediatric Cardiology, Mayo Clinic, Rochester, Minnesota, [‡]Department of Cardiovascular and Respiratory Medicine, Shiga University of Medical Sciences, Seta-tsukinowa, Otsu, Japan, and [§]Division of Cardiology, University of Ottawa Heart Institute, Ottawa, Ontario, Canada.

BACKGROUND Type 1 long QT syndrome (LQT1) is caused by loss-of-function mutations in the *KCNQ1*-encoded Kv7.1 channel that conducts the slowly activating component of the delayed rectifier K^+ current (I_{Ks}). Clinically, the diagnosis of LQT1 is complicated by variable phenotypic expressivity, whereby approximately 25% of genotype-positive individuals present with concealed LQT1 (resting corrected QT [QTc] interval $\leq$460 ms).

OBJECTIVE To determine whether a specific molecular mechanism contributes to concealed LQT1.

METHODS We identified a multigenerational LQT1 family whereby 79% of the patients genotype-positive for p.Ile235Asn-*KCNQ1* (I235N-Kv7.1) have concealed LQT1. We assessed the effect I235N-Kv7.1 has on I_{Ks} and the ventricular action potential (AP) by using in vitro analysis and computational simulations.

RESULTS Clinical data showed that all 10 patients with I235N-Kv7.1 have normal resting QTc intervals but abnormal QTc interval prolongation during the recovery phase of an electrocardiographic treadmill stress test. Voltage-clamping HEK293 cells coexpressing wild-type Kv7.1 and I235N-Kv7.1 (to mimic the patients' genotypes) showed that I235N-Kv7.1 generated relatively normal functioning Kv7.1 channels but were insensitive to protein kinase A (PKA) activation. Phosphomimetic and quinidine sensitivity studies suggest that I235N-Kv7.1 limits the conformational changes in Kv7.1 channels, which are necessary to upregulate I_{Ks} after PKA phosphorylation. Computational ventricular AP simulations predicted that the PKA insensitivity of I235N-Kv7.1 is primarily responsible for prolonging the AP with β-adrenergic stimulation, especially at slower cycle lengths.

CONCLUSIONS *KCNQ1* mutations that generate relatively normal Kv7.1 channels, but limit the upregulation of I_{Ks} by PKA activation, likely contribute to concealed LQT1.

KEYWORDS Long QT syndrome; *KCNQ1*; Kv7.1; PKA activation; I_{Ks}; Treadmill stress test

ABBREVIATIONS **AKAP9** = A-kinase anchoring protein 9 (Yotiao); **AP** = action potential; **APD_{90}** = steady-state action potential duration at 90% repolarization; **ECG** = electrocardiogram/electrocardiographic; **HEK293** = human embryonic kidney 293; **I_{Ks}** = slowly activating delayed rectifier K^+ current; **I_{MAX}** = maximally activated **I_{Ks}**; ***k*** = slope factor; **LQT1** = type 1 long QT syndrome; **LQTS** = long QT syndrome; **PKA** = protein kinase A; **QTc** = corrected QT; **$V_{½}$** = midpoint potential for half-maximal activation of I_{Ks}; **WT** = wild-type Kv71.

(Heart Rhythm 2014;11:459–468)

Introduction

Congenital long QT syndrome (LQTS) is a condition of abnormal cardiac repolarization that affects approximately 1 of every 2000 live births and is characterized clinically by prolongation of the heart rate–corrected QT (QTc) interval on a resting 12-lead electrocardiogram (ECG). Patients with LQTS are at an increased risk of syncope, seizures, and

This work was supported by the American Heart Association predoctoral award PRE7370003 (to Dr Bartos) and the National Heart Lung and Blood Institute grants R01 HL087039 (to Dr Delisle) and F30 HL106993 (to Dr Giudicessi). Dr Ackerman is a consultant for Biotronik, Boston Scientific, Medtronic, St Jude Medical, and Transgenomic. In addition, there is a license agreement between Transgenomic and Mayo Clinic Health Solutions and royalties are distributed in accordance with the Mayo Clinic policy. **Address reprint requests and correspondence:** Dr Brian P. Delisle, Department of Physiology, University of Kentucky College of Medicine, 800 Rose St, MS508, Lexington, KY 40536. E-mail address: brian.delisle@uky.edu.

1547-5271/$-see front matter http://dx.doi.org/10.1016/j.hrthm.2013.11.021

sudden cardiac death secondary to polymorphic ventricular tachyarrhythmias.[1] Type 1 long QT syndrome (LQT1) is caused by loss-of-function missense, nonsense, frameshift, or splice-site altering mutations in the *KCNQ1*-encoded Kv7.1 α subunit and accounts for an estimated 40% of all genotype-positive LQTS cases.[1–4] Kv7.1 α subunits tetramerize to form the pore of the slowly activating delayed rectifier K^+ current (I_{Ks}) channel complex, and in the human heart, I_{Ks} is upregulated by protein kinase A (PKA) activation to prevent ventricular action potential (AP) prolongation during β-adrenergic stimulation.[5,6] Consequently, many patients with LQT1 tend to experience life-threatening symptoms while exercising or swimming.[7,8] Unfortunately, rendering a diagnosis of LQT1 on the basis of a 12-lead ECG alone presents a significant challenge as an estimated 25% of genotype-positive individuals with LQT1 fail to display an abnormal QTc interval at rest, commonly referred to as a concealed LQT1 phenotype.[9,10]

Patients with a concealed LQTS phenotype may remain at risk of cardiac events during exercise owing to inappropriate adaptation of repolarization.[11] As such, developing a deeper understanding of the molecular mechanisms underlying a concealed LQT1 phenotype might improve personalized diagnostic and management approaches to lower the risk of life-threatening arrhythmias. In this study, we tested the hypothesis that some mutations contribute to a high incidence of the concealed LQT1 phenotype by a specific molecular mechanism.

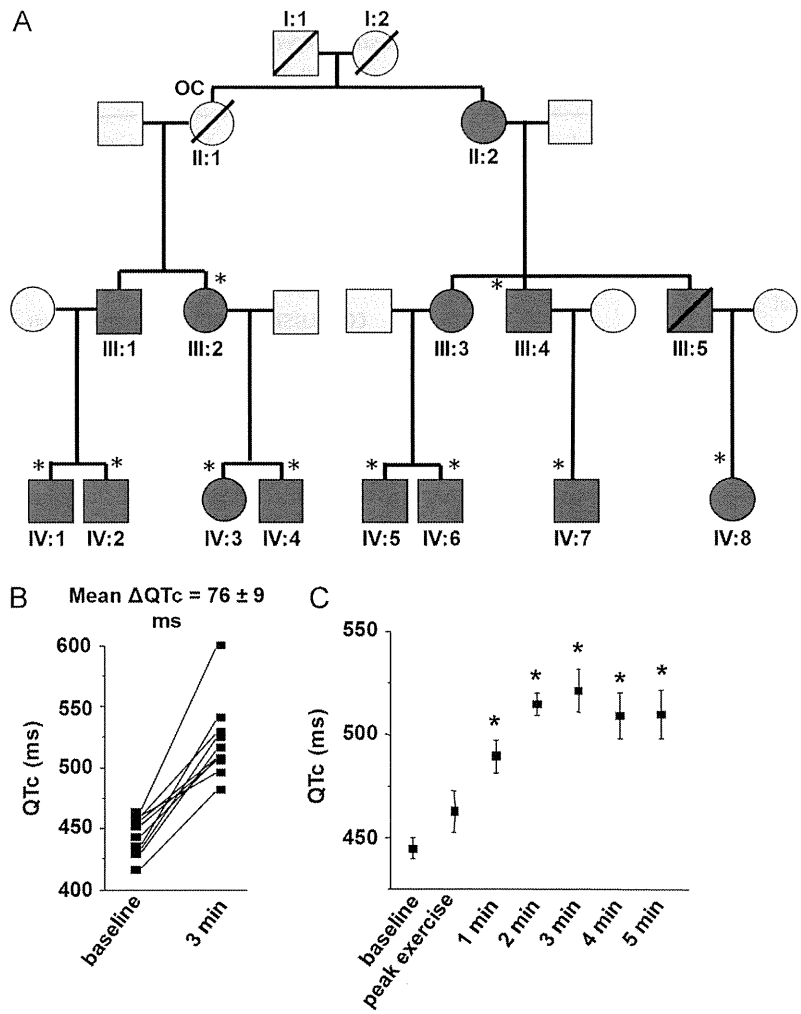

Figure 1 I235N-Kv7.1 causes concealed LQT1. **A:** A pedigree of a LQT1 family with I235N-Kv7.1 who underwent an ECG treadmill stress test. Patients with the I235N-Kv7.1 mutation are denoted by filled gray symbols. Individual males and females are denoted by squares and circles, respectively; each generation is denoted by a Roman numeral; OC denotes an obligate carrier; and asterisks signify individuals who underwent an ECG treadmill stress test. **B:** The QTc interval values recorded at baseline and after 3 minutes of recovery used to calculate ΔQTc of the 10 patients positive for I235N-Kv7.1 who underwent an ECG treadmill stress test are plotted. **C:** The mean QTc interval values recorded during the exercise treadmill stress test were plotted at baseline, peak exercise, and 1, 2, 3, 4, or 5 minutes during the recovery phase ($^*P < .05$ vs baseline). ECG = electrocardiogram; LQT1 = type 1 long QT syndrome; QTc = corrected QT; ΔQTc = difference in QTc interval between baseline recording and 3 minutes after the ECG treadmill stress test.

Methods

Identification of a concealed LQT1 multigenerational pedigree

In this institutional review board–approved study, a retrospective review of more than 1000 individuals with a referral diagnosis of LQTS evaluated at Mayo Clinic between 1998 and 2008 was used to identify 76 of 249 (30.5%) individuals with LQT1 who featured a concealed LQTS electrocardiographic phenotype at rest (defined as a QTc interval of $\leq$460 ms for both men and women).[12] To identify the mutation(s) most likely to confer a mutation-specific risk of concealed LQTS, we further limited this list to LQT1 pedigrees in which $\geq$2 genotype-positive family members featured a concealed LQTS phenotype. This process led to the identification of 3 moderate-to-large LQT1 pedigrees harboring I235N-Kv7.1, Y315C-Kv7.1, and T322A-Kv7.1.[12] The concealed LQT1 phenotype was observed in 15 of 19 (79%) individuals who are genotype positive for I235N-Kv7.1, 4 of 7 (57%) individuals who are genotype positive for Y315C-Kv7.1, and 4 of 9 (44%) individuals who are genotype positive for T322A-Kv7.1. Given the electrophysiological defects associated with Y315C-Kv7.1[13] and T322A-Kv7.1[14] have been described in detail previously and these mutations showed a lower incidence of concealed LQT1, we focused our investigation on the large LQT1 family harboring the I235N-Kv7.1 mutation. Resting 12-lead and exercise stress test ECGs were analyzed manually, and the QT interval (lead II or V_5) was corrected for heart rate by using Bazett's formula (QTc interval = $QT/\sqrt{RR}$) as described previously.[12,15]

Genetic analysis, mutagenesis, electrophysiology, computational modeling, and statistics

These methods were performed similarly as described previously and are explained in detail in the Online Supplement.[16–19]

Results

Patients with LQT1 and the I235N-Kv7.1 mutation show marked QTc prolongation during the recovery phase of the ECG treadmill stress test

Ten members of the large I235N-Kv7.1 LQT1 pedigree who underwent a treadmill stress test are depicted in Figure 1A. Each of these patients had a bona fide LQT1 phenotype as evident by the normal QTc interval at rest (Table 1) and ΔQTc > 30 ms at 3 minutes during the recovery phase as compared to baseline (Table 1 and Figure 1B).[12] Moreover, marked QTc interval prolongation was seen at all recovery time points tested (Figure 1C), which suggested that I235N-Kv7.1 confers a mutation-specific risk of concealed LQT1. Importantly, genotype-positive patients are at risk of life-threatening cardiac events, as illustrated by the near drowning of the index case at age 15 (IV.8) and the suspicious sudden death of her genotype-positive father at age 41 (III.5).

Table 1 Clinical characteristics of the genotype-positive I235N-Kv7.1 family

Genotype-positive patients, n (female, n)	15 (6)
ECG treadmill stress test, n (female, n)	10 (3)
Mean age ± SD (y)	38 ± 14
Female mean age ± SD (y)	46 ± 19
Male mean age ± SD (y)	35 ± 11
Mean resting QTc ± SD (ms)	445 ± 16
Female mean resting QTc ± SD (ms)	441 ± 24
Male mean resting QTc ± SD (ms)	446 ± 14
Mean resting HR ± SD (ms)	76 ± 17
Female mean resting HR ± SD (ms)	74 ± 8
Male mean resting HR ± SD (ms)	76 ± 19
Mean ΔQTc ± SD (ms)	76 ± 29
Female mean ΔQTc ± SD (ms)	88 ± 40
Male mean ΔQTc ± SD (ms)	71 ± 25
Near-drowning episode, n (female, n)	1 (1)
Mean 3 min of recovery HR ± SD (ms)	117 ± 16
Female mean 3 min of recovery HR ± SD (ms)	115 ± 7
Male mean 3 min of recovery HR ± SD (ms)	118 ± 18

ECG = electrocardiogram; HR = heart rate; QTc = corrected QT; ΔQTc = difference between the baseline QTc interval and the QTc interval measured at 3 minutes during the recovery phase after the ECG treadmill stress test.

I235N-Kv7.1 disrupts a highly conserved amino acid in S4 and causes a large reduction in I_{Ks} that is largely normalized by the coexpression of wild-type Kv7.1

The Kv7.1 α subunit is composed of cytosolic amino and carboxy termini and 6 transmembrane segments (S1–S6; Figure 2A). I235 is located in S4 between highly conserved positively charged amino acids critical for the voltage dependence of Kv channel gating (Figure 2B).[20] Sequence alignments show that I235 is also conserved in other Kv α subunits (Figure 2B).[20] We tested whether I235N-Kv7.1 generates a unique functional phenotype that accounts for the high incident of the concealed LQT1 clinical phenotype. For all voltage-clamping experiments, we coexpressed the K^+ channel β subunit, KCNE1, which is obligatory for Kv7.1 to generate native-like I_{Ks} currents.[2,3] I_{Ks} was recorded from cells expressing wild-type Kv7.1 (WT), I235N-Kv7.1, or coexpressing WT and I235N-Kv7.1 (to mimic the patients' genotypes) by applying steplike pulses from −80 to 70 mV in 10-mV increments for 5 seconds, immediately followed by applying a "tail" pulse to −50 mV for 5 seconds (Figure 2C). The peak I_{Ks} amplitude recorded during the step pulse or at the start of the tail pulse was plotted as a function of the step pulse potential (Figures 2D–2E). These data show that cells expressing WT conducted I_{Ks}-like currents; cells expressing I235N-Kv7.1 generated small I_{Ks} that activated at positive potentials; and cells coexpressing WT and I235N-Kv7.1 conducted I_{Ks} that was slightly smaller than cells expressing WT. We calculated changes in the maximally activated I_{Ks} (I_{MAX}) and tested for changes in gating by fitting the individual tail I_{Ks}-V relations with a Boltzmann equation (Table 2A and Figure 2E). I_{Ks} measured from cells expressing I235N-Kv7.1 without WT were too small to be reliably described by a Boltzmann equation and

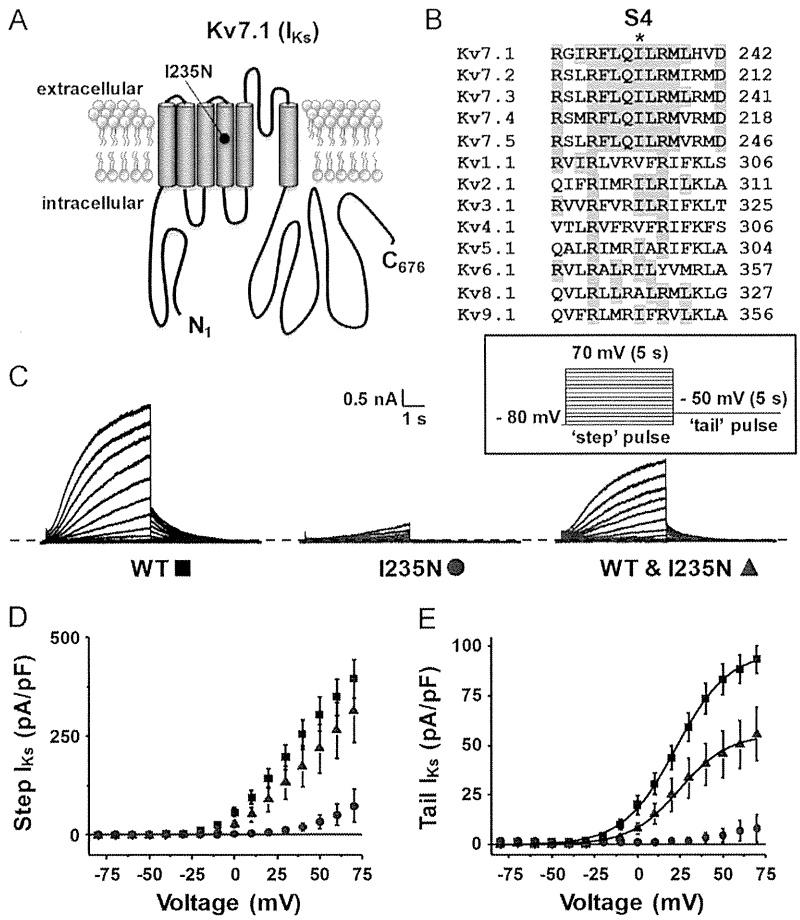

Figure 2 I235N-Kv7.1 disrupts a conserved amino acid residue in S4 and coexpression of WT mostly corrects the loss of function caused by I235N-Kv7.1. **A:** Membrane topology of a single Kv7.1 pore-forming α subunit embedded in the plasma membrane. **B:** Amino acid residue sequence alignments for the S4 of Kv7.1 (NP_055194.1), Kv7.2 (NP_742105), Kv7.3 (NP_004510), Kv7.4 (NP_004691.2), Kv7.5 (NP_001153606), Kv1.1 (NP_000208.2), Kv2.1 (NP_004966), Kv3.1 (NP_001106212), Kv4.1 (NP_004970), Kv5.1 (NP_002227), Kv6.1 (NP_002228), Kv9.1 (NP_002242.2), and Kv10.1 (NP_002229.1). Amino acid residues conserved with Kv7.1 are shaded gray. **C:** Representative traces of whole-cell I_{Ks} measured from HEK293 cells transfected WT, I235N-Kv7.1, or WT and I235N-Kv7.1 complementary DNA. **D and E:** The mean peak (panel D) step or (panel E) tail I_{Ks} is plotted as a function of the step voltage for cells expressing WT (n = 11; black squares), I235N-Kv7.1 (n = 8; gray circles), or WT and I235N-Kv7.1 (n = 9; gray triangles). I_{Ks} = slowly activating delayed rectifier K^+ current; WT = wild-type Kv7.1.

were excluded from analyses. The mean Boltzmann data showed that compared with cells expressing WT, cells coexpressing WT and I235N-Kv7.1 caused a ~30% reduction in I_{MAX} with modestly different gating properties (a slightly more positive midpoint potential for half-maximal activation of I_{Ks} [$V_{½}$] and shallower slope factor [*k*]). Together, these data demonstrate that the coexpression of WT largely corrected the loss of function caused by I235N-Kv7.1.

Cells coexpressing WT and I235N-Kv7.1 generate PKA-insensitive I_{Ks}

An important functional role of I_{Ks} is to shorten the ventricular AP in response to β-adrenergic stimulation. β-adrenergic stimulation activates PKA, which increases I_{Ks} by phosphorylating Kv7.1 at S27.[5,21] We previously showed that the *KCNQ1* mutation R231H-Kv7.1, which is 4 amino acid residues upstream of I235, is insensitive to PKA activation.[16] Therefore, we tested whether cells coexpressing WT and I235N-Kv7.1 might also generate PKA-insensitive I_{Ks}. We used a similar voltage protocol as in Figure 2C and measured I_{Ks} before and after the perfusion of forskolin and IBMX (Figure 3A). All these experiments were performed with the coexpression of KCNE1 and A-kinase anchoring protein 9 (Yotiao; AKAP9), which is the A-kinase anchoring protein important for coupling PKA to the I_{Ks} channel complex.[5,21,22] The peak I_{Ks} amplitude recorded at the start of the tail pulse was plotted as a function of the step pulse potential and described with a Boltzmann equation (Table 2B and Figures 3B–3C). These data show that PKA activation in cells expressing WT increased I_{MAX}. However, it did not increase I_{MAX} in cells coexpressing WT and I235N-Kv7.1. I235N-Kv7.1 appears to prevent the upregulation of I_{Ks} through PKA activation.

Table 2 Electrophysiological properties of I235N-Kv7.1 described by using the Boltzmann equation

Kv7.1 (n)	I_{MAX} (pA/pF)	$V_{½}$(mV)	*k* (mV/e-fold Δ)
A.Basal			
WT (11)	83.53 ± 5.82	20.00 ± 3.68	13.61 ± 1.61
WT and I235N-Kv7.1 (12)	57.03 ± 8.26*	36.36 ± 5.57*	19.70 ± 2.20*
B.Before (-) or after (+) forskolin & IBMX			
WT (-) (6)	73.99 ± 6.67	13.21 ± 3.82	9.55 ± 1.37
WT (+)	112.70 ± 12.46*	3.62 ± 6.13	12.72 ± 1.29
WT and I235N-Kv7.1 (-) (6)	48.55 ± 7.47†	28.83 ± 3.10*†	17.32 ± 1.87
WT and I235N-Kv7.1 (+)	58.11 ± 10.75†	30.25 ± 4.79*†	20.95 ± 1.65
C. Phosphomimetic			
S27A (5)	83.42 ± 7.79	20.73 ± 4.55	11.12 ± 1.52
S27D (5)	140.8 ± 7.86*	22.68 ± 3.40	13.33 ± 0.96
S27A and S27A/I235N (7)	69.18 ± 10.97†	39.00 ± 2.81	15.74 ± 0.91
S27D and S27D/I235N (9)	92.83 ± 9.58†	38.12 ± 5.84	16.76 ± 1.88

A: To determine I_{MAX}, $V_{½}$, and *k*, the peak tail I_{Ks}-V relations were described by using the Boltzmann equation for cells expressing WT or WT and I235N-Kv7.1 (gray line; Figure 2E; $^*P < .05$ vs WT). **B:** Cells expressing WT or WT and I235N-Kv7.1 (gray line; Figures 3B and 3C) before (−) or after (+) perfusion of forskolin and IBMX ($^*P < .05$ vs WT before perfusion; $^\dagger P < .05$ vs WT after perfusion). **C:** Cells expressing S27A-Kv7.1, S27D-Kv7.1, S27A- and S27A/I235N-Kv7.1, or S27D- and S27D/I235N-Kv7.1 (gray line; Figures 4B and 4C; $^*P < .05$ vs S27A; $\dagger P < .05$ vs S27D).

I235N-Kv7.1 blunts the increase in I_{Ks} caused by the phosphomimetic substitution of S27D

I235N-Kv7.1 might prevent PKA stimulation of I_{Ks} by inhibiting phosphorylation at S27. To test this, we introduced amino acid residue substitutions at S27 in WT or I235N-Kv7.1 that prevent or mimic S27 phosphorylation (S27A or S27D, respectively).[5,22] We recorded I_{Ks} from cells expressing S27A-Kv7.1 or S27D-Kv7.1 and from cells coexpressing S27A- and S27A/I235N-Kv7.1 or S27D- and S27D/I235N-Kv7.1 by using the same voltage protocol as in Figure 2C (Figure 4A). Boltzmann analyses of the tail I_{Ks}-V relations showed that as compared with cells expressing S27A-Kv7.1, cells expressing S27D-Kv7.1 had a larger I_{MAX} but did not alter $V_{½}$ or *k* (Table 2C and Figures 4B–4C).

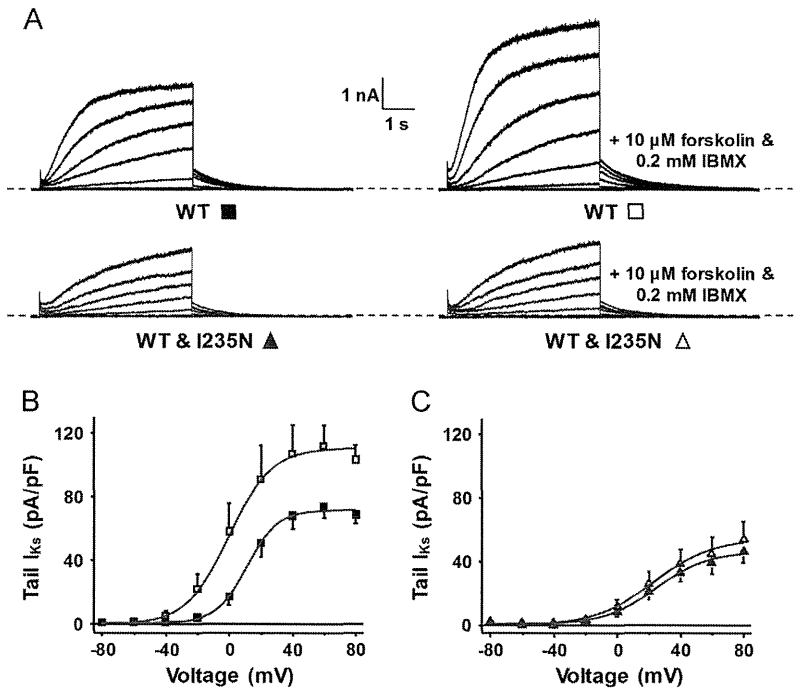

Figure 3 I235N-Kv7.1 generates PKA-insensitive Kv7.1 channels. (**A**) Representative traces of whole-cell I_{Ks} measured from cells transfected with WT or WT and I235N-Kv7.1 complementary DNA before and after extracellular perfusion of 10 µM of forskolin and 0.2 mM of IBMX. The mean peak tail I_{Ks}-V relations are plotted for cells expressing (**B**) WT (n = 6) before (black squares) and after (black open squares) perfusion or (**C**) WT and I235N-Kv7.1 (n = 6) before (triangles) and after (open triangles) perfusion. I_{Ks} = slowly activating delayed rectifier K^+ current; PKA = protein kinase A; WT = wild-type Kv7.1.

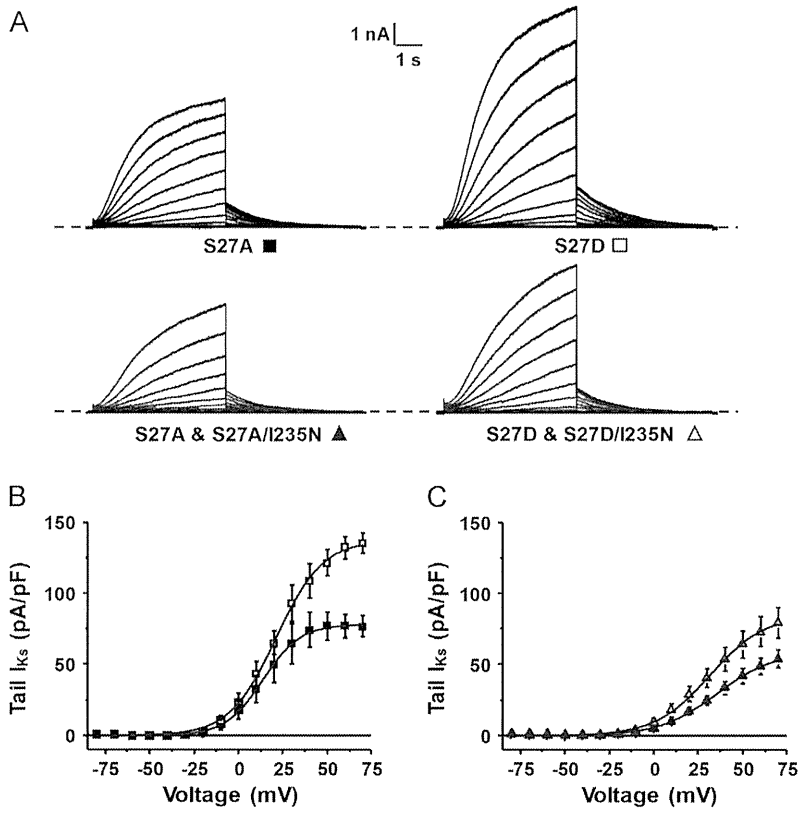

Figure 4 The phosphomimetic substitution of S27D does not increase the functional expression of I235N-Kv7.1. **A:** Representative traces of whole-cell I_{Ks} measured from cells transfected with S27A- or S27D-Kv7.1, and S27A- and S27A/I235N-Kv7.1 or S27D- and S27D/I235N-Kv7.1 complementary DNA. **B and C:** The mean peak tail I_{Ks}-V relations are plotted for cells expressing (panel B) S27A-Kv7.1 (n = 5; black squares) or S27D-Kv7.1 (n = 5; open squares) and (panel C) S27A- and S27A/I235N-Kv7.1 (n = 7; gray triangles) or S27D- and S27D/I235N-Kv7.1 (n = 9, open triangles). I_{Ks} = slowly activating delayed rectifier K^+ current.

In contrast, cells coexpressing S27D-Kv7.1 and S27D/I235N-Kv7.1 blunted the increase in I_{MAX} as compared with cells coexpressing S27A- and S27A/I235N-Kv7.1. These data suggest that S27D does not upregulate I_{Ks} in channels with the I235N-Kv7.1 mutation.

Since the phosphomimetic mutation did not rescue the upregulation of I_{Ks}, we tested whether I235N-Kv7.1 prevents the necessary conformational changes in Kv7.1 channels required to upregulate I_{Ks} after PKA activation. Previous studies by Yang and colleagues[23,24] showed that PKA-stimulated Kv7.1 channels or S27D-Kv7.1 reduce quinidine block of I_{Ks} compared with nonstimulated Kv7.1 channels. These data suggest that the PKA phosphorylation of S27 or S27D cause conformational changes in Kv7.1 channels that increase I_{Ks} and restricts the access of quinidine to its binding site.[25] In other words, the relative sensitivity of I_{Ks} to quinidine block is a good indicator of the conformational changes associated with S27 phosphorylation and the phosphomimetic substitution of S27D. We compared the % block of I_{Ks} caused by quinidine from cells expressing S27A-Kv7.1, S27D-Kv7.1, or S27D- and S27D/I235N-Kv7.1 (Figure 5). Similar to what was shown previously, cells expressing S27D-Kv7.1 conducted I_{Ks} that was less

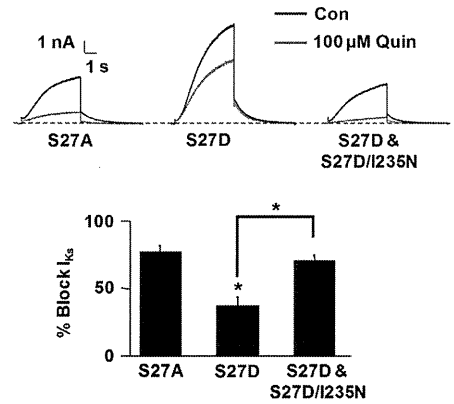

Figure 5 I235N-Kv7.1 preserves the sensitivity of I_{Ks} to quinidine block. Representative I_{Ks} traces before (black) and after the perfusion of 100 µM quinidine (Quin; red) measured from cells transfected with S27A-Kv7.1, S27D-Kv7.1, or S27D- and S27D/I235N-Kv7.1 complementary DNA. I_{Ks} was recorded by applying a step pulse to 50 mV for 5 seconds followed by applying a tail pulse to −50 mV for 5 seconds. The mean % block of the peak tail I_{Ks} are plotted ($^*P < .05$). I_{Ks} = slowly activating delayed rectifier K^+ current.

sensitive to quinidine block than cells expressing S27A-Kv7.1. However, cells coexpressing S27D- and S27D/I235N-Kv7.1 conducted I_{Ks} and demonstrated sensitivity to quinidine block similar to that shown by cells expressing S27A-Kv7.1. Together, these data suggest that I235N-Kv7.1 prevents the PKA upregulation of I_{Ks} by limiting the conformational changes in Kv7.1 channels associated with S27 phosphorylation.

Computational simulations of ventricular AP with or without β-adrenergic stimulation suggest that I_{Ks} insensitivity to PKA is primarily responsible for a ventricular AP prolongation

Next, we wanted to test how I235N-Kv7.1 might alter the duration of a ventricular AP over a wide range of cycle lengths with or without β-adrenergic stimulation by using computational modeling.[18] To mimic the effects that I235N-Kv7.1 has on I_{Ks}, the I_{Ks} component was reduced by 30% and made insensitive to PKA. We compared these simulations with control simulations or simulations that simply reduced the I_{Ks} component by 30% (without changing PKA sensitivity). The steady-state action potential duration at 90% repolarization (APD_{90}) at cycle lengths ranging from 300 to 1000 ms was calculated. In the absence of β-adrenergic stimulation, a 30% reduction in I_{Ks} resulted in a 1%–2% prolongation of the APD_{90} between 300 and 1000 ms (Figures 6A–6C). The presence of β-adrenergic stimulation indicated that reducing the I_{Ks} component by 30% still increased the APD_{90} by only 1%–2%. However, reducing the I_{Ks} component by 30% and making it PKA-insensitive increased the APD_{90} from 6% to 10% at cycle lengths between 300 and 1000 ms. These computational data suggest that the PKA insensitivity of I235N-Kv7.1 is primarily responsible for the concealed LQT1 phenotype.

The data from the LQTS patient registry indicate that dominant-negative LQT1 mutations, which decrease total I_{Ks} by $>50\%$, are an independent risk factor for life-threatening events.[26] We used computational modeling to assess the pathological/clinical relevance of PKA-insensitive vs dominant-negative Kv7.1 mutations. We compared simulations in which I_{Ks} was PKA-insensitive, a simulation that mimicked a dominant-negative LQT1 mutation (the I_{Ks} component was reduced by 70%), or a simulation that mimicked a PKA-insensitive dominant-negative LQT1 mutation. During simulations in which the I_{Ks} component was only PKA-insensitive, the APD_{90} increased with β-adrenergic stimulation by 6%–8%. A dominant-negative I_{Ks} simulation increased the APD_{90} by 3%–4% in the basal simulations and by 6%–8% in β-adrenergic simulations for cycle lengths 300–1000 ms (Figures 6D–6E). Coupling the PKA insensitivity with a dominant-negative reduction in I_{Ks} increased the APD_{90} by 8%–12% for cycle lengths 300–1000 ms. These data suggest that PKA-insensitive Kv7.1 mutations, which do not reduce basal I_{Ks}, can prolong the AP as much as dominant-negative Kv7.1 mutations in conditions of β-adrenergic stimulation. We conclude that assessing the PKA sensitivity of seemingly normal functioning Kv7.1 mutations is critical to determine their pathological significance.

Discussion

The increasing availability of clinical genetic testing for LQTS promises to one day allow for the development of personalized approaches to the prevention of life-threatening arrhythmias in individuals afflicted with this genetic disorder. However, the probabilistic interpretation of LQTS genetic testing results is complicated by the observation that 4%–8% of the ostensibly healthy individuals are expected to harbor rare amino acid–altering genetic variants in 1 of 3 major LQTS-susceptibility genes (*KCNQ1*, *KCNH2*, and *SCN5A*).[27] In addition, it is estimated that approximately 25% of the individuals with an LQTS-causative mutation fail to manifest any abnormalities in their QTc interval on resting ECG (ie, concealed LQTS).[11] There remain few insights into the genetic and/or electrophysiological mechanisms that underlie concealed LQTS phenotypes.[26,28] The fact that individuals with a concealed LQTS phenotype still have a >10-fold higher relative risk of sudden cardiac arrest/death than their genotype-negative relatives highlights the pressing need to develop a deeper understanding of the mechanisms underlying this phenomenon.[27] Therefore, the purpose of this study was to determine whether a specific molecular mechanism contributes to the concealed LQT1 phenotype.

In this study, we identified a large LQT1 multigenerational pedigree whereby the vast majority of individuals who were genotype-positive for I235N-Kv7.1 displayed a concealed LQT1 phenotype. The family was brought to clinical attention owing to a near-drowning episode of the I235N-positive index case and the sudden unexpected death of her genotype-positive father. Therefore, we directly evaluated the functional properties of I235N-Kv7.1 in HEK293 cells. While homomeric I235N-Kv7.1 caused a severe loss of function, the coexpression of WT markedly improved the dysfunctional I_{Ks} phenotype. These data contradict a recent report by Henrion et al,[29] who previously suggested that I235N-Kv7.1 causes dominant-negative suppression of WT when expressed in *Xenopus laevis* oocytes. Although we cannot completely account for this discrepancy, we suspect that it might be due in part to the alternative expression system used.[30,31]

The activation of the β-adrenergic receptor initiates a signaling cascade through $G_{\alpha s}$ proteins that activate adenylate cyclase to increase intracellular levels of cyclic adenosine monophosphate cAMP. cAMP activates PKA, and PKA phosphorylates several substrate proteins in cardiomyocytes, specifically phosphorylating S27 on the N terminus of Kv7.1, which upregulates I_{Ks}.[5] These data suggest that patients with LQT1 who have dominant-negative LQT1 mutations ($>50\%$ reduction in I_{Ks}) that generate Kv7.1 channels insensitive to PKA activation are likely to manifest a severe clinical phenotype. For example, Heijman et al[22] and Barsheshet et al[32] reported several dominant-negative

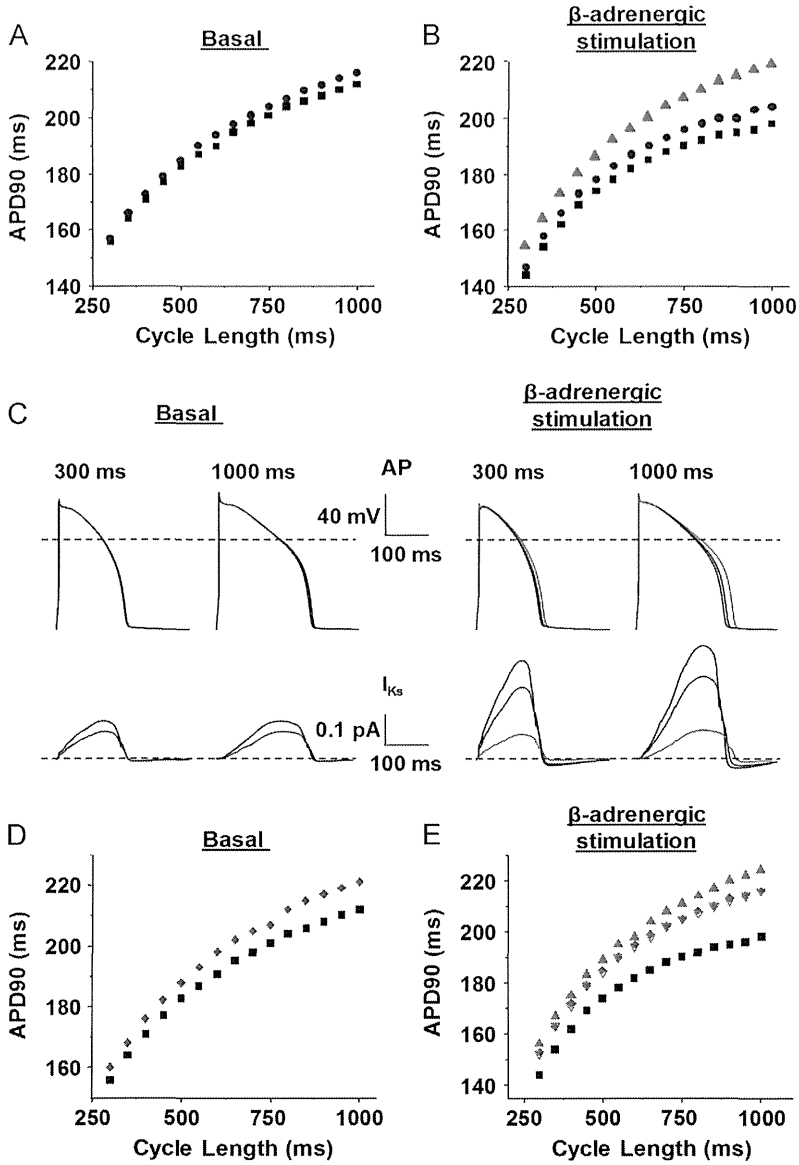

Figure 6 Computational simulations suggest that making the I_{Ks} component insensitive to PKA selectively increases the ventricular AP duration with β-adrenergic stimulation. The APD_{90} was plotted as a function of the cycle length. Shown are the APD_{90} calculated at cycle lengths between 300 and 1000 ms for control simulations (black squares), simulations in which the I_{Ks} component was reduced by 30% (blue circles), and simulations in which the I_{Ks} component was reduced by 30% and made insensitive to PKA (red triangles) (**A**) for basal conditions or (**B**) with β-adrenergic stimulation. (**C**) Representative AP waveforms and the corresponding I_{Ks} for control simulations (black line), simulations in which the I_{Ks} component was reduced by 30% (blue line), and simulations in which the I_{Ks} component was reduced by 30% and rendered PKA-insensitive (red line) for 300 or 1000 ms. The black and red AP waveforms are not visible for the basal simulations because they are overlaid by the blue AP waveform, and the red I_{Ks} is not visible for the basal simulations because it is overlaid by the blue I_{Ks}. To mimic dominant-negative I_{Ks} suppression, simulations were repeated for control I_{Ks} (black squares) or in which the I_{Ks} component was reduced by 70% (aqua diamonds) for (**D**) basal conditions or (**E**) β-adrenergic stimulation. Also shown are simulations in which I_{Ks} is only PKA-insensitive (orange open inverted triangles) or is reduced by 70% and PKA-insensitive (gold triangles). AP = action potential; APD_{90} = steady-state action potential duration at 90% repolarization; I_{Ks} = slowly activating delayed rectifier K^+ current; PKA = protein kinase A.

LQT1-linked mutations that generate PKA-insensitive Kv7.1 channels and associate with severe clinical phenotypes. Most recently, Wu et al[33] showed that a mildly dominant-negative LQT1-linked mutation (G269S-Kv7.1) primarily contributes to an adrenergic-induced LQTS phenotype. We now show that I235N-Kv7.1, which does not cause dominant-negative effect on I_{Ks} but generates PKA-insensitive Kv7.1 channels, contributes to a high incidence of the concealed LQT1 phenotype. Computational ventricular AP simulations that incorporate the functional effects of I235N-Kv7.1 suggest that the mild dysfunctional phenotype minimally alters the AP duration in basal conditions, but β-adrenergic

stimulation, especially at slow cycle lengths, unmasks AP prolongation similar to a dominant-negative LQT1 mutation. The exacerbated prolongation of the ventricular AP duration at slower cycle lengths qualitatively mimics the changes in the QTc interval during the exercise treadmill stress test for patients with I235N-Kv7.1 (QTc prolongation was exacerbated as the heart rate slows during the recovery phase of the ECG stress test).

Although an increasing number of LQT1-linked mutations are being linked to PKA insensitivity, the molecular mechanisms for most PKA-insensitive mutations have not been fully elucidated. The suppression of I_{Ks} upregulation has previously been reported in an LQT1-linked mutation G589D-Kv7.1, which disrupts the binding of AKAP9 to the C terminus.[5] Heijman et al[22] showed that A341V-Kv7.1 prevents I_{Ks} upregulation through PKA activation by inhibiting the phosphorylation at S27. Unlike A341V-Kv7.1, the phosphomimetic substitution of S27 in I235N-Kv7.1 did not increase I_{Ks}. Moreover, phosphomimetic I235N-Kv7.1 generated I_{Ks} that maintained a high sensitivity to quinidine block. Recently, Yang et al[25] performed extensive Kv7.1 mutagenesis and molecular modeling to examine the mechanism for quinidine block. These studies suggest that quinidine allosterically inhibits I_{Ks} by binding to an intracellular pocket generated by amino acid residues in the S4–S5 linker and S6, which raises the intriguing possibility that S27 phosphorylation causes a conformational change that upregulates I_{Ks} and alters the quinidine binding pocket to decrease quinidine block. The presence of I235N-Kv7.1 prevents both PKA-induced conformational changes and I_{Ks} upregulation. These data identify a novel mechanism by which LQT1 mutations generate PKA-insensitive Kv7.1 channels.

Study limitations

This study has several limitations. The data were obtained in a widely used heterologous expression system that might not completely recapitulate in vivo phenotypes. Additional family specific factors, including *KCNQ1* polymorphisms in the 3′ allele, might contribute to the concealed LQT1 phenotype in this family.[34]

Conclusions

Our study suggests that the exercise treadmill stress test for patients with concealed LQT1 might help identify patients who harbor PKA-insensitive Kv7.1 channels. To our knowledge, these are the first data that link PKA insensitivity to an abnormal QT response during the ECG exercise treadmill stress test. Future studies incorporating the exercise treadmill stress test combined with mutation-specific risk assessment will likely improve the treatment of each patient with LQT1. We conclude that some PKA-insensitive LQT1 mutations, which generate relatively mild dysfunctional phenotypes in basal conditions, can contribute to a high penetrance of the concealed LQT1 phenotype.

Acknowledgments

We thank Dr Robert Kass (Columbia University, New York, NY) for providing the AKAP9 plasmid DNA.

Appendix

Supplementary data

Supplementary data associated with this article can be found in the online version at http://dx.doi.org/10.1016/j.hrthm.2013.11.021.

References

1. Crotti L, Celano G, Dagradi F, Schwartz PJ. Congenital long QT syndrome. Orphanet J Rare Dis 2008;3:18.
2. Barhanin J, Lesage F, Guillemare E, Fink M, Lazdunski M, Romey G. K(V)LQT1 and IsK (minK) proteins associate to form the I(Ks) cardiac potassium current. Nature 1996;384:78–80.
3. Sanguinetti MC, Curran ME, Zou A, et al. Coassembly of K(V)LQT1 and minK (IsK) proteins to form cardiac I(Ks) potassium channel. Nature 1996;384:80–83.
4. Wang Q, Curran ME, Splawski I, et al. Positional cloning of a novel potassium channel gene: KVLQT1 mutations cause cardiac arrhythmias. Nat Genet 1996;12:17–23.
5. Marx SO, Kurokawa J, Reiken S, et al. Requirement of a macromolecular signaling complex for beta adrenergic receptor modulation of the KCNQ1-KCNE1 potassium channel. Science 2002;295:496–499.
6. Volders PG, Stengl M, van Opstal JM, et al. Probing the contribution of IKs to canine ventricular repolarization: key role for beta-adrenergic receptor stimulation. Circulation 2003;107:2753–2760.
7. Schwartz PJ, Priori SG, Spazzolini C, et al. Genotype-phenotype correlation in the long-QT syndrome: gene-specific triggers for life-threatening arrhythmias. Circulation 2001;103:89–95.
8. Choi G, Kopplin LJ, Tester DJ, Will ML, Haglund CM, Ackerman MJ. Spectrum and frequency of cardiac channel defects in swimming-triggered arrhythmia syndromes. Circulation 2004;110:2119–2124.
9. Priori SG, Napolitano C, Schwartz PJ. Low penetrance in the long-QT syndrome: clinical impact. Circulation 1999;99:529–533.
10. Giudicessi JR, Ackerman MJ. Determinants of incomplete penetrance and variable expressivity in heritable cardiac arrhythmia syndromes. Transl Res 2013;161:1–14.
11. Goldenberg I, Horr S, Moss AJ, et al. Risk for life-threatening cardiac events in patients with genotype-confirmed long-QT syndrome and normal-range corrected QT intervals. J Am Coll Cardiol 2011;57:51–59.
12. Horner JM, Horner MM, Ackerman MJ. The diagnostic utility of recovery phase QTc during treadmill exercise stress testing in the evaluation of long QT syndrome. Heart Rhythm 2011;8:1698–1704.
13. Bianchi L, Priori SG, Napolitano C, et al. Mechanisms of I(Ks) suppression in LQT1 mutants. Am J Physiol Heart Circ Physiol 2000;279:H3003–H3011.
14. Burgess DE, Bartos DC, Reloj AR, et al. High-risk long QT syndrome mutations in the Kv7.1 (KCNQ1) pore disrupt the molecular basis for rapid K(+) permeation. Biochemistry 2012;51:9076–9085.
15. Giudicessi JR, Ackerman MJ. Prevalence and potential genetic determinants of sensorineural deafness in KCNQ1 homozygosity and compound heterozygosity. Circ Cardiovasc Genet 2013;6:193–200.
16. Bartos DC, Anderson JB, Bastiaenen R, et al. A KCNQ1 mutation causes a high penetrance for familial atrial fibrillation. J Cardiovasc Electrophysiol 2013;24:562–569.
17. Bartos DC, Duchatelet S, Burgess DE, et al. R231C mutation in KCNQ1 causes long QT syndrome type 1 and familial atrial fibrillation. Heart Rhythm 2011;8:48–55.
18. Soltis AR, Saucerman JJ. Synergy between CaMKII substrates and beta-adrenergic signaling in regulation of cardiac myocyte Ca(2+) handling. Biophys J 2010;99:2038–2047.
19. Tester DJ, Will ML, Ackerman MJ. Mutation detection in congenital long QT syndrome: cardiac channel gene screen using PCR, dHPLC, and direct DNA sequencing. Methods Mol Med 2006;128:181–207.
20. Papazian DM, Timpe LC, Jan YN, Jan LY. Alteration of voltage-dependence of Shaker potassium channel by mutations in the S4 sequence. Nature 1991;349:305–310.
21. Kurokawa J, Motoike HK, Rao J, Kass RS. Regulatory actions of the A-kinase anchoring protein Yotiao on a heart potassium channel downstream of PKA phosphorylation. Proc Natl Acad Sci U S A 2004;101:16374–16378.

22. Heijman J, Spatjens RL, Seyen SR, et al. Dominant-negative control of cAMP-dependent IKs upregulation in human long-QT syndrome type 1. Circulation Res 2012;110:211–219.
23. Yang T, Kanki H, Zhang W, Roden DM. Probing the mechanisms underlying modulation of quinidine sensitivity to cardiac I(Ks) block by protein kinase A-mediated I(Ks) phosphorylation. Br J Pharmacol 2009;157:952–961.
24. Yang T, Kanki H, Roden DM. Phosphorylation of the IKs channel complex inhibits drug block: novel mechanism underlying variable antiarrhythmic drug actions. Circulation 2003;108:132–134.
25. Yang T, Smith JA, Leake BF, Sanders CR, Meiler J, Roden DM. An allosteric mechanism for drug block of the human cardiac potassium channel KCNQ1. Mol Pharmacol 2013;83:481–489.
26. Moss AJ, Shimizu W, Wilde AA, et al. Clinical aspects of type-1 long-QT syndrome by location, coding type, and biophysical function of mutations involving the KCNQ1 gene. Circulation 2007;115:2481–2489.
27. Kapa S, Tester DJ, Salisbury BA, et al. Genetic testing for long-QT syndrome: distinguishing pathogenic mutations from benign variants. Circulation 2009;120:1752–1760.
28. Giudicessi JR, Kapplinger JD, Tester DJ, et al. Phylogenetic and physicochemical analyses enhance the classification of rare nonsynonymous single nucleotide variants in type 1 and 2 long-QT syndrome. Circ Cardiovasc Genet 2012;5:519–528.
29. Henrion U, Strutz-Seebohm N, Duszenko M, Lang F, Seebohm G. Long QT syndrome-associated mutations in the voltage sensor of I(Ks) channels. Cell Physiol Biochem 2009;24:11–16.
30. Furutani M, Trudeau MC, Hagiwara N, et al. Novel mechanism associated with an inherited cardiac arrhythmia: defective protein trafficking by the mutant HERG (G601S) potassium channel. Circulation 1999;99:2290–2294.
31. Nakajima T, Furukawa T, Hirano Y, et al. Voltage-shift of the current activation in HERG S4 mutation (R534C) in LQT2. Cardiovasc Res 1999;44:283–293.
32. Barsheshet A, Goldenberg I, O-Uchi J, et al. Mutations in cytoplasmic loops of the KCNQ1 channel and the risk of life-threatening events: implications for mutation-specific response to beta-blocker therapy in type 1 long-QT syndrome. Circulation 2012;125:1988–1996.
33. Wu J, Naiki N, Ding W-G, et al. A molecular mechanism for adrenergic-induced long QT syndrome. J Am Coll Cardiol 2013.
34. Amin AS, Giudicessi JR, Tijsen AJ, et al. Variants in the 3′ untranslated region of the KCNQ1-encoded Kv7.1 potassium channel modify disease severity in patients with type 1 long QT syndrome in an allele-specific manner. Eur Heart J 2012;33:714–723.

A Kir3.4 mutation causes Andersen–Tawil syndrome by an inhibitory effect on Kir2.1

Yosuke Kokunai, MD, PhD*
Tomohiko Nakata, MD*
Mitsuru Furuta, MD*
Souhei Sakata, PhD
Hiromi Kimura, MD, PhD
Takeshi Aiba, MD, PhD
Masao Yoshinaga, MD, PhD
Yusuke Osaki, MD
Masayuki Nakamori, MD, PhD
Hideki Itoh, MD, PhD
Takako Sato, MD, PhD
Tomoya Kubota, MD, PhD
Kazushige Kadota, MD, PhD
Katsuro Shindo, MD, PhD
Hideki Mochizuki, MD, PhD
Wataru Shimizu, MD, PhD
Minoru Horie, MD, PhD
Yasushi Okamura, MD, PhD
Kinji Ohno, MD, PhD
Masanori P. Takahashi, MD, PhD

Correspondence to Dr. Takahashi: mtakahas@neurol.med.osaka-u.ac.jp

Supplemental data at Neurology.org

ABSTRACT

Objective: To identify other causative genes for Andersen-Tawil syndrome, which is characterized by a triad of periodic paralysis, cardiac arrhythmia, and dysmorphic features. Andersen-Tawil syndrome is caused in a majority of cases by mutations in *KCNJ2*, which encodes the Kir2.1 subunit of the inwardly rectifying potassium channel.

Methods: The proband exhibited episodic flaccid weakness and a characteristic TU-wave pattern, both suggestive of Andersen-Tawil syndrome, but did not harbor *KCNJ2* mutations. We performed exome capture resequencing by restricting the analysis to genes that encode ion channels/associated proteins. The expression of gene products in heart and skeletal muscle tissues was examined by immunoblotting. The functional consequences of the mutation were investigated using a heterologous expression system in *Xenopus* oocytes, focusing on the interaction with the Kir2.1 subunit.

Results: We identified a mutation in the *KCNJ5* gene, which encodes the G-protein-activated inwardly rectifying potassium channel 4 (Kir3.4). Immunoblotting demonstrated significant expression of the Kir3.4 protein in human heart and skeletal muscles. The coexpression of Kir2.1 and mutant Kir3.4 in *Xenopus* oocytes reduced the inwardly rectifying current significantly compared with that observed in the presence of wild-type Kir3.4.

Conclusions: We propose that *KCNJ5* is a second gene causing Andersen-Tawil syndrome. The inhibitory effects of mutant Kir3.4 on inwardly rectifying potassium channels may account for the clinical presentation in both skeletal and heart muscles. ***Neurology*® 2014;82:1058–1064**

GLOSSARY

cRNA = complementary RNA; **LQT** = long QT; **SNP** = single nucleotide polymorphism; **SNV** = single nucleotide variant.

Periodic paralysis is a heterogeneous disorder caused by mutations in several ion channel genes, including sodium, calcium, and potassium channels.[1–3] Andersen–Tawil syndrome is a form of periodic paralysis that is characterized by a triad of periodic muscle weakness, cardiac arrhythmia, and dysmorphic features.[4,5] Although dominantly inherited, its phenotypes are highly variable and its penetrance is low.[6,7] The syndrome has been proposed as LQT7; however, the ECG features are distinct from those of classic forms of long QT (LQT) syndrome, i.e., characteristic TU patterns, including enlarged U waves, a wide TU junction, and a prolonged terminal T-wave downslope.[6,8]

KCNJ2 mutation, which encodes the Kir2.1 subunit, causes Andersen–Tawil syndrome.[9] Kir2.1 is predominantly expressed in the brain, heart, and skeletal muscles and forms an inwardly rectifying potassium channel via the homo- or heteromeric assembly of 4 Kir2.x subunits.[10] Most *KCNJ2* mutations cause loss of function or dominant-negative suppression of the inwardly rectifying

*These 3 authors contributed equally to this work.

From the Department of Neurology (Y.K., M.F., M.N., T.K., H.M., M.P.T.), and Laboratory of Integrative Physiology, Department of Physiology (S.S., Y. Okamura), Osaka University Graduate School of Medicine, Suita, Osaka; Division of Neurogenetics (T.N., K.O.), Center for Neurological Diseases and Cancer, Nagoya University Graduate School of Medicine, Nagoya, Aichi; Department of Cardiovascular and Respiratory Medicine (H.K., H.I., M.H.), Shiga University of Medical Science, Otsu, Shiga; Division of Arrhythmia and Electrophysiology (T.A., W.S.), Department of Cardiovascular Medicine, National Cerebral and Cardiovascular Center, Suita, Osaka; Department of Pediatrics (M.Y.), National Hospital Organization Kagoshima Medical Center, Kagoshima; Department of Neurology (Y. Osaki, K.S.), Kurashiki Central Hospital, Kurashiki, Okayama; Department of Legal Medicine (T.S.), Osaka Medical College, Takatsuki, Osaka; Department of Cardiology (K.K.), Kurashiki Central Hospital, Kurashiki, Okayama; and Department of Cardiovascular Medicine (W.S.), Nippon Medical School, Bunkyo, Tokyo, Japan. Y.K. is currently affiliated with the Department of Neurology, Osaka General Medical Center, Sumiyoshi, Osaka, Japan; and T.K. is currently affiliated with the Department of Biochemistry and Molecular Biology, Division of Biological Sciences, The University of Chicago, IL.

Go to Neurology.org for full disclosures. Funding information and disclosures deemed relevant by the authors, if any, are provided at the end of the article.